An inverse modelling technique for glass forming by gravity sagging

Y. Agnon [a] Y.M. Stokes [b],*

[a]*Department of Civil and Environmental Engineering, Technion, Israel Institute of Technology, 32000 Haifa, Israel.*

[b]*Applied Mathematics, School of Mathematical Sciences, University of Adelaide, 5005 Australia.*

Abstract

Some optical surfaces are formed by gravity sagging of molten glass. A glass sheet supported on a ceramic former is heated; the glass becomes a very viscous fluid and sags under its own weight until the lower surface is in full contact with the former. The smooth upper free surface is the required optical surface. Its shape is dependent on the initial geometry and, in optical terms, differs significantly from the former shape. The inverse problem is to determine the shape of the former that produces a prescribed upper surface. This is a difficult, highly nonlinear problem. A finite element algorithm has been developed to compute gravity sagging for any given initial geometry (the forward problem). The present work describes a successful iterative method, which uses the output from a number of forward problems to determine the required former shape.

Key words: Inverse problem, creeping flow, free surface, glass forming

1 Introduction

Thermal replication is a process used in the production of aspheric optical components as described in [9,12] and shown in Figure 1. A glass workpiece or pre-form is placed on a ceramic former which has been previously machined to a given shape. This combination is heated in an oven so that the glass melts and sags, or 'slumps', under its own weight into the former. On cooling the glass component is removed from the former. Its lower surface is rough due to

* Corresponding author. Tel.: +61-8-8303-4808; fax: +61-8-8303-3696.
  Email address: ystokes@maths.adelaide.edu.au (Y.M. Stokes).

(a) Before slumping; with geometrical notation.

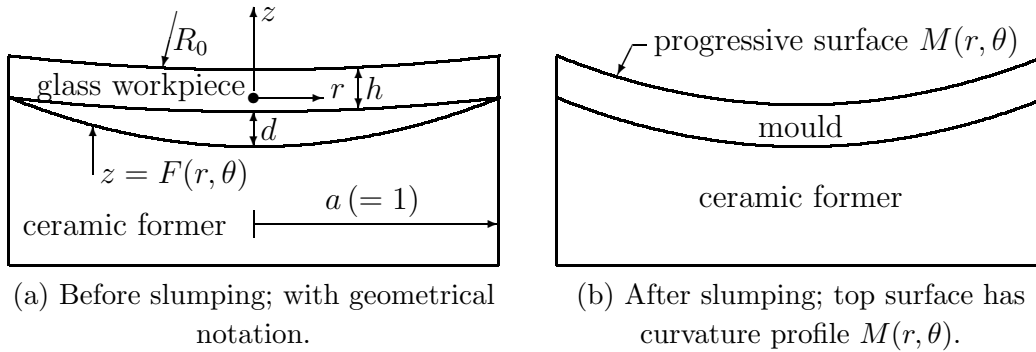(b) After slumping; top surface has curvature profile $M(r, \theta)$.

Fig. 1. The thermal replication process.

contact with the rough former, but the upper surface is smooth and may be used, for example, as a mirror surface or as a mould surface for casting plastic ophthalmic lenses; the curvature of this surface must meet the design criteria to sufficient optical precision. The process takes its name from the idea of 'replicating' the basic shape of the ceramic former on the upper glass surface while smoothing out any small scale imperfections in the former surface arising from machining. However, the transfer of even the basic former shape to the glass is not exact, especially in terms of surface curvature which is the quantity of primary interest for optical components.

This is an example of a highly nonlinear inverse problem. The process designer must determine the geometry of the former and pre-form and the temperature-time profile to yield the required product; the product designer must ensure that the product is achievable by thermal replication. Solving this inverse problem is much more difficult than solving the forward problem of determining the product yielded by a given geometrical setup and temperature-time history.

Such inverse problems are important in industrial forming processes. They arise, for example, in the manufacture of automotive windscreens [3,5], in thermoforming of plastics [1,2,14,20] and in forging [7,13,21], to name a few which appear in the literature. For these examples temperature is an important control on the product being produced and much of the literature is concerned with inverse methods for determining suitable temperature profiles in space and time [1,2,5,11,20]. In relation to geometrical controls, work on shape optimisation of an initial workpiece or preform includes [13,14] while [7,21] consider the optimisation of die shape design to minimise forming load and achieve deformation uniformity respectively. This paper presents a method for determining mould (or former) shapes to yield a desired product shape. While we specifically focus on thermal replication of optical components, the method described has more general applicability.

It is generally accepted that molten glass may be modelled as a very viscous Newtonian fluid [10]; non-Newtonian behaviour is important in only relatively

2

few situations (see, for example, [6]). In the problem of present interest the flow is very slow with a time scale of hours. Working temperatures are around 700°C with glass viscosity μ of the order of 10^6 Pa.s. Slumping velocities scale like $\rho g a^2 / \mu$, where $\rho \sim 2500\,\mathrm{kg/m}^3$, g and a are density, gravitational acceleration and a typical length scale, respectively. Here the length scale a is the pre-form radius, about 45 mm. Then, the Reynolds number $\rho^2 g a^3 / \mu^2 \sim 6 \times 10^{-6}$ is very small and, as in many other glass-forming processes [4,8,18,19], we are justified in neglecting the inertial terms in the Navier-Stokes equation and solving the Newtonian creeping-flow (or Stokes flow) equations

$$-\nabla p + \nabla \cdot (\mu \nabla \mathbf{u}) - \rho g \, \mathbf{k} = 0$$

together with the continuity equation

$$\nabla \cdot \mathbf{u} = 0,$$

where p and $\mathbf{u}$ are pressure and velocity respectively, and $\mathbf{k}$ is the unit vector pointing vertically up.

We are also justified in neglecting surface tension, since the Capillary number is large, scaling as $\rho g a^2 / \sigma$, where $\sigma \approx 0.3\,\mathrm{N/m}$ is the coefficient of surface tension for glass. Thus we must solve the creeping-flow equations subject to no-slip conditions ($\mathbf{u} = \mathbf{0}$) where the molten glass is in contact with a solid boundary, and zero-stress and kinematic conditions on the free-surface boundaries elsewhere.

Thermal replication clearly involves heat flow in addition to fluid flow. However, the glass-former combination is heated in a closed oven in which spatial temperature variations over distances comparable to the pre-form diameter are small, so that we may assume that the temperature, and hence the viscosity μ, in the glass is a function of time t only. Further, as explained in [17] a consequence of using a creeping-flow model is that temporal changes in the viscosity affect only the slump time, but not the final product. Then, we may effectively account for a time-varying viscosity within the time scale and, for a given constant value of the dimensionless slump time

$$T = \rho g \int \frac{1}{\mu(t)} dt,$$

the shape of the optical surface resulting from a given initial geometrical setup is determined by solving for the flow of the molten glass assuming a constant viscosity, such that $T = \rho g t / \mu$; there is no need to solve a coupled heat and fluid flow problem.

Solution of the forward problem of determining the top surface shape of the glass for a given (axisymmetric) former shape and initial pre-form geometry is discussed in detail in [15–17] and we give just a brief summary of the methods

used here. The Newtonian creeping-flow equations are solved in the glass, subject to no-slip where the glass is in contact with the former and zero-stress conditions on free surfaces, using a finite-element method. Lagrangian time-stepping is used to track the changing geometry of the glass over time. At the end of the process, when the lower surface of the glass workpiece is in full contact with the ceramic former, the curvature profile of the upper surface is computed using a least-squares quintic B-spline fit to surface coordinate data. We assume here that the forward problem is solved satisfactorily in this way.

We are, therefore, left with the inverse problem: to determine the geometrical setup to give the required optical surface. Both the former and preform shapes influence the final outcome, but the former shape is by far the most important control and adjusting its shape the best mechanism for modifying the optical surface. Our primary focus is therefore on determining former shape. At present this is done by a time-consuming, iterative experimental procedure and we here propose a computational approach which can be used to investigate the range of surface profiles that can be made by thermal replication and which may be developed into a tool that can replace experiments and reduce process design time.

2 Notation

We consider a glass disc pre-form of radius a, thickness h and initial radius of curvature R_0, and a former of radius a, with cavity surface described in terms of elevation $z = F(r, \theta)$ such that there is a maximum distance d between the former and the lower pre-form surface, as shown in Figure 1. We shall work in cylindrical polar coordinates (r, θ, z) where $z = 0$ is the plane of support of the glass. Next, we non-dimensionalise using a as the length scale, equivalent to setting $a = 1$. Then h becomes the aspect ratio of the pre-form and d the aspect ratio of the former cavity. The desired curvature profile on the top surface of the glass is $K(r, \theta)$, while the actual curvature profile after slumping is $M(r, \theta)$.

We here restrict our attention to axisymmetric geometries, although we use notation applicable to general three-dimensional problems to which our methods are, in principle, readily extended. Then we may use the symmetry of the problem and restrict our computational domain to one radius of the geometry. Information supplied by the industry indicates that the glass thickness is such that $0.04 \leq h \leq 0.15$ covers the full range of possibilities for the pre-form aspect ratio, while $0.01 \leq d \leq 0.10$ is a suitable parameter range for the aspect ratio of the former cavity; R_0, the initial curvature of the pre-form, is chosen so that d does not exceed this range. Typically $h = 0.1333$ and $d = 0.0444$. Unless otherwise stated, we use $R_0 = \infty$ corresponding to a flat pre-form.

3 A zeroth-order solution

A zeroth-order estimate of the transfer function from former to glass is obtained assuming that, at the end of the slumping process, the glass forms a layer of uniform thickness h over the former surface $F(r, \theta)$. Such a simple shift function is not sufficiently accurate for optical products where the curvature is important. Rather, the transfer function is a complex function that has nonlinear dependence on geometrical parameters, such as the depth of the mould and the thickness of the pre-form.

The solution method we will describe is based on approximate linear superposition, starting from an initial estimate of the solution such as provided by the zeroth-order solution and, hence, we begin by looking more closely at this solution. We note that curvature is itself a nonlinear function $(z''/(1 + z'^2)^{3/2}$, where z is surface elevation and primes denote differentiation with respect to r) and, strictly, cannot be obtained by superposition. However, the slope of the surfaces considered are small, so that the curvature is almost identical with the second derivative of the surface which can be obtained by linear superposition. Hence we will use the second derivative everywhere in place of curvature, while retaining the name "curvature", although we could also use the curvature function itself since the error introduced is small relative to other components of the error.

Suppose that we wish to obtain a constant curvature on the glass by slumping into a spherically shaped former. Then, to zeroth-order we expect the curvature of the top glass surface to be constant at $K = 1/(R_f - h)$, where $R_f = (1 + d^2)/(2d)$ is the radius of curvature of the former. Let K be the desired curvature profile. The error $E(r, \theta)$ is the difference between the actual surface curvature M and the desired curvature, i.e. $E = M - K$, and $|E|$ is constrained by some industry-prescribed tolerance function. Usually, the tolerance is smaller at the centre and increases towards the edge. Since the glass is edge trimmed after slumping, we need only be concerned with E over some range $0 \leq r < b$, $b < a$, although to minimise waste it is desirable that b be as close to the glass and former radius a as possible.

Noting that both d and h are typically small, we may write

$$K = \frac{2d}{1 + d^2 - 2dh} \approx 2d, \tag{1}$$

from which we might expect the actual curvature profile M to be, not only near constant, but also reasonably linearly dependent on the aspect ratio of the former cavity d and independent of h. Thus we might expect there to be a function $f(r) \approx 2$ such that $M(r)/d \approx f(r)$.

Figure 2 shows the scaled curvature profile $M(r)/d$ for different values of $d \in [0.01, 0.10]$ and for a flat pre-form of fixed aspect ratio $h = 0.1333$; the solution of the forward problem was taken when full contact of the lower glass surface with the mould had been attained, which occurs at different times for the different formers. We see that, in the central region $r < 0.1$ and near the edge $r > 0.6$, M/d varies from two by an amount greater than can be accounted for by the approximation (1). Also, we note that M/d reduces to almost the same curve in the central region of the disc, showing that M increases almost linearly with d in this region for each of the four cases considered. However, elsewhere M depends on d in a more nonlinear manner.

Figure 3 shows the effect of the pre-form aspect ratio on the scaled curvature M/d for slumping into a former with cavity aspect ratio $d = 0.05$; for this figure the solution to the forward problem was taken at the same time for each of the cases considered and when there was full contact of the lower glass surface with the former. Clearly, the deviation of M from (1) is quite dependent on h and the smaller h the better is the approximation $M/d = 2$. For the thinnest glass $h = 0.05$, the top surface curvature profile is noticeably less smooth than the curves for the thicker pre-forms. We believe this to be due to mould roughness (due to a piecewise linear mould representation) and/or roughness resulting from contact events between the glass and former, which is not sufficiently smoothed out when the glass is thin.

It is evident that the inaccuracy of the zeroth-order method for determining the former profile F to yield a desired curvature profile K on the glass increases with both the cavity aspect ratio of the former d and the aspect ratio of the pre-form h. Not unexpectedly, thinner glass more accurately replicates the former curvature; but defects in the former surface are more likely to be transferred to the glass also. Since a sufficiently thick glass pre-form must be used to damp out small-scale imperfections in the former, our task is to devise a method for modifying the former profile to reduce the curvature error E, given the pre-form aspect ratio h.

4   Former modification: linearised approach

The idea used is essentially that of the multivariable Newton-Raphson method. Our zeroth-order method gives an estimate of the former elevation profile $z = F(r, \theta)$ for a given desired curvature $K(r, \theta)$ on the top surface of the glass. On slumping we find that the actual curvature profile is $M(r, \theta)$. We denote this
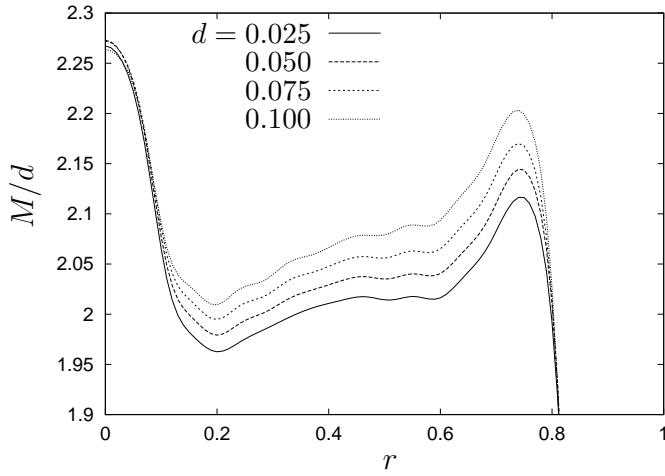
$$F(r, \theta) \Rightarrow M(r, \theta).$$

Fig. 2. M/d for a glass pre-form of aspect ratio $h = 0.1333$ slumping into spherical formers of different cavity aspect ratio d. The curves were computed after full mould contact at times $t = 0.075, 0.100, 0.125, 0.150$ for $d = 0.025, 0.050, 0.075, 0.100$ respectively.
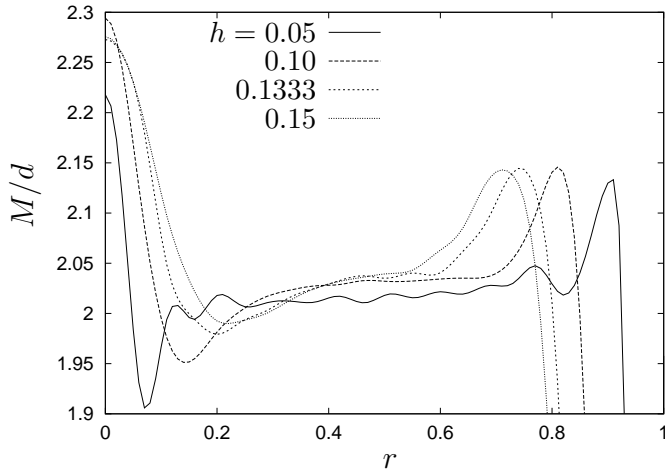

Fig. 3. M/d for glass pre-forms of different aspect ratio h slumping into a spherical former with cavity aspect ratio $d = 0.05$. The curves were all computed at time $t = 0.100$ by which time full mould contact had been established in each case.

If M is sufficiently close to K then

$$K(r, \theta) = M(r, \theta) + \delta M(r, \theta),$$

where δM is a small perturbation of M, and we need to find a small perturbation δF of F such that

$$F(r, \theta) + \delta F(r, \theta) \Rightarrow M(r, \theta) + \delta M(r, \theta).$$

We define δM to be the *target* and δF to be the *solution*. Now, we may solve the forward problem for each of a 'basis' set of m former perturbations $\delta_i(r, \theta)$, $i = 1, m$, and determine the corresponding glass surface perturbations

$\mu_i(r, \theta), i = 1, m$, i.e.

$$F(r, \theta) + \delta_i(r, \theta) \Rightarrow M(r, \theta) + \mu_i(r, \theta).$$

Then, assuming a (nearly) linear response we have

$$F(r, \theta) + \sum_{i=1}^{m} \alpha_i \delta_i(r, \theta) \Rightarrow M(r, \theta) + \sum_{i=1}^{m} \alpha_i \mu_i(r, \theta),$$

and we need only determine the coefficients α_i such that

$$\delta M(r, \theta) \approx \sum_{i=1}^{m} \alpha_i \mu_i(r, \theta).$$

These are found by taking $J \geq m$ collocation points r_j, $j = 1, J$, in the region of interest $(0 \leq r \leq b)$, and determining the best-least-squares solution to the resulting $J \times m$ system of equations. The solution is then given by

$$\delta F(r, \theta) = \sum_{i=1}^{m} \alpha_i \delta_i(r, \theta),$$

and the new former shape is $\tilde{F} = F + \delta F$. Setting $F = \tilde{F}$ we may repeat this procedure, iterating until M is sufficiently close to K, i.e. $|E| = |-\delta M|$ is sufficiently small over $0 \leq r \leq b$, or until we are unable to reduce the error any further.

Now, we may think of the former perturbation as being comprised of a (possibly infinite) linear combination of Fourier components, i.e. $\delta F = \sum_i \alpha_i \delta_i$ with each of the δ_i contributing a component of a different wavenumber. A small wavenumber (long wavelength) former perturbation δ_i is expected to produce an essentially small wavenumber perturbation μ_i on the glass, so that the target δM can be similarly considered as a Fourier series. Assuming that the target is a well-behaved function, small wavenumber components will be of larger amplitude and more linear than larger wavenumber components and should be determined first and removed from the target to give a new target comprised of the larger wavenumber components. Hence, we adopt an iterative approach. We first rank the δ_i from smallest to largest wavenumber. Then at iteration m we use the above described procedure with the set of former perturbations δ_i, $i = 1, m$. From the solution δF obtained we obtain a new former and a new target to be used at iteration $m + 1$. This new target is, essentially, comprised of Fourier components μ_i, $i > m$ of larger wavenumber than already considered, having a solution comprised of Fourier components δ_i, $i > m$. The physics of slumping, which is designed to smooth out small scale perturbations on the former, also supports this iterative approach and indicates that there will be a limit on the size and amplitude of perturbation that can be used effectively.

8

5   Orthogonalisation

The success or otherwise of this procedure depends firstly on obtaining a sufficiently good initial estimate of F, and this is yielded by the zeroth-order approximation method. Secondly, the procedure requires a set of former-perturbation functions δ_i and, at each iteration m, a set of coefficients α_i, $i = 1, m$ such that

(a) for the given δ_i, the α_i fall within the linear response range for the $(m-1)$th (i.e. the previous) state which we shall denote by (F_{m-1}, M_{m-1}), i.e.

$$F_{m-1} + \sum_{i=1}^{m} \alpha_i \delta_i \Rightarrow M_{m-1} + \sum_{i=1}^{m} \alpha_i \mu_i$$

or

(b) there is at most one $\alpha_j \approx 1$, $1 \leq j \leq m$, and the coefficients $\tilde{\alpha}_i = \alpha_i$, $i \neq j$, $\tilde{\alpha}_j = \alpha_j - 1$ fall within the linear response range for the state $(F_{m-1} + \delta_j, M_{m-1} + \mu_j)$, i.e.

$$(F_{m-1} + \delta_j) + \sum_{i=1}^{m} \tilde{\alpha}_i \delta_i \Rightarrow (M_{m-1} + \mu_j) + \sum_{i=1}^{m} \tilde{\alpha}_i \mu_i.$$

Because of the iterative approach, adding one additional perturbation δ_m to the set at iteration m, we fully expect $j = m$.

If we are fortunate enough to find a set of δ_i such that, at iteration m, $\alpha_m \approx 1$ then the δ_i and resulting μ_i need not behave linearly in the usual way. With our present solution method, the contribution to the target from μ_m is largely removed from the target (excepting for a contribution due to nonlinearity) at the mth iteration at which δ_m is added to the set of δ_i. Thus, if things are 'linear enough', at the mth iteration we expect that the contribution to the target from μ_m will be dominant, with only quite small contributions from μ_i, $i = 1, m - 1$ which should therefore be in the linear range.

We can facilitate this by orthgonalising the glass perturbations μ_i, $i = 1, m$ at each iteration m. Let ν_i be the set of orthogonalised glass perturbations derived from the μ_i, and γ_i be the corresponding set of former perturbations derived from the δ_i. We let $\nu_1 = \mu_1$ and $\gamma_1 = \delta_1$. Then, for i ranging from 2 to m, we generate the other γ_i, ν_i using a Gramm-Schmidt process:

(i) $\nu_i \Leftarrow \mu_i, \quad \gamma_i \Leftarrow \delta_i.$

(ii) $\nu_i \Leftarrow \nu_i - \dfrac{(\nu_i \cdot \nu_j)\nu_j}{\|\nu_j\|}, \quad \gamma_i \Leftarrow \gamma_i - \dfrac{(\nu_i \cdot \nu_j)\gamma_j}{\|\nu_j\|}, \qquad j = 1, \ldots, (i-1).$

(iii) $\delta_i \Leftarrow \gamma_i$

(iv) $F + \delta_i \Rightarrow M + \mu_i$

Note that having obtained new former perturbations δ_i at (iii) we must slump again using these at (iv) to find the corresponding glass perturbations μ_i, which are therefore not exactly orthogonal. We may iterate to improve orthogonality, the trade-off being the large amount of computing time that this involves. However, we can check orthogonality as we proceed and perform only as many iterations as necessary. For the cases considered herein, one to three were used.

Our final algorithm incorporating all of the features discussed to date is given in Appendix A.

6   Linearity of response

Since the effectiveness of our solution method depends on the validity of our linearity assumptions, we next explore the issue of linearity.

For this we consider a pre-form of aspect ratio $h = 0.1333$ slumping into a former which has cavity surface elevation $z = F + \delta_i$, where $z = F(r, \theta)$ defines a spherical cavity surface with cavity aspect ratio $d = 0.05$ and δ_i is a small perturbation of this surface. Let us consider the set of small perturbations

$$\delta_i = \frac{\epsilon}{2} \left(1 + (-1)^{i+1} \cos(i \pi r)\right), \quad i = 1, 2, \ldots, \tag{2}$$

where ϵ is a small number determining the amplitude of the perturbation and $i = 2/\lambda$ is the number of wavelengths of length λ across the diameter of the former, i.e. $k = i\pi = 2\pi/\lambda$ is the wavenumber. The functions δ_i have the property of zero perturbation of the former at its edge $r = 1$, which is taken as a fixed reference. Then linearity of the response demands that

$$F + (\alpha \delta_i + \beta \delta_j) \Rightarrow M + \mu_{i,\alpha;j,\beta},$$

where

$$\mu_{i,\alpha;j,\beta} = \mu_{i,\alpha} + \mu_{j,\beta} = \alpha \mu_i + \beta \mu_j,$$

after a fixed slump time, which we take to be a little more than the time for the glass to achieve full contact with the unperturbed former.

We first consider multiplicative linearity by setting $\beta = 0$ and, for values of i and ϵ, compute the response $\mu_{i,\alpha}$ for perturbations $\alpha \delta_i$ for various values α. Linearity demands that $\mu_{i,\alpha} = \alpha \mu_i$ and hence can be measured by computing $e_N = \mu_{i,\alpha} - \alpha \mu_i$. Then for a given i we need to determine a value of ϵ and the range of values of α such that $|e_N|$ is small. Because the glass is edge trimmed, we are not concerned too much with nonlinearity near the edge and may focus attention on the inner region. In fact these linearity computations will give an indication of the amount of edge trim required. We shall notionally allow
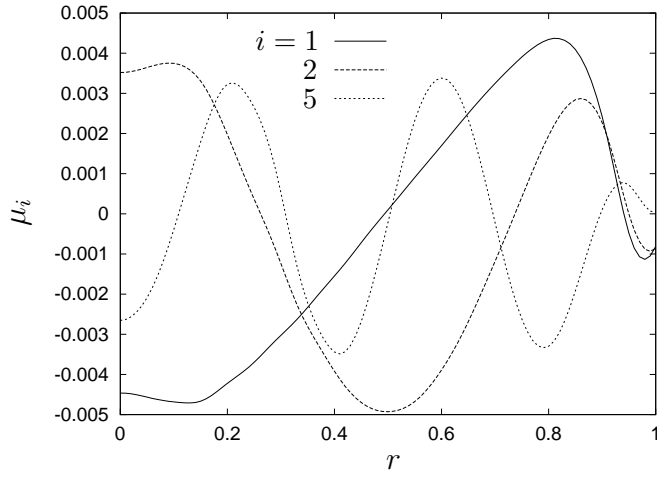
10

Fig. 4. Slumping of a pre-form of aspect ratio $h = 0.1333$ into a base spherical mould with $d = 0.05$ at $t = 0.1$. Response μ_i to former perturbations δ_i with $\epsilon = 0.001/i^2$ for $i = 1, 2, 5$.
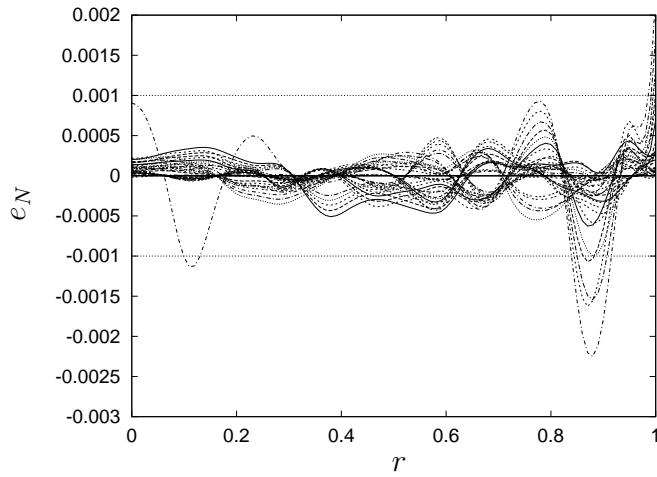

Fig. 5. Slumping of a pre-form of aspect ratio $h = 0.1333$ into a base spherical mould with $d = 0.05$ at $t = 0.1$. Error $e_N = \mu_{i,\alpha} - \alpha\mu_i$ for $i = 1, 2, 5$ and $\alpha = \pm 1, \pm 6, \pm 7, \ldots, \pm 10$.

$|e_N| \sim 0.001$, based on very approximate information from the industry and noting that the permissible tolerance varies greatly with position on the lens mould. For this reason and because of the iterative nature of our method, this is not a rigid tolerance and more nonlinearity may be permissible in some areas and/or a tighter tolerance in others.

After some experimenting, we have found $\epsilon = 0.001\, i^{-2}$ to be a suitable scaling for δ_i. The i^{-2} factor is not too surprising, since it cancels the i^2 factor in the former curvature perturbation function $\delta_i'' = (i\pi)^2(-1)^{i+2}(\epsilon/2)\cos(i\pi r)$ and hence keeps the magnitude of the former curvature perturbation (and hence that of the glass curvature) from growing with the wavenumber of the perturbation. Figure 4 shows the curvature perturbations μ_i resulting from former perturbations δ_i, $i = 1, 2, 5$, and Figure 5 shows the error due to nonlinearity

11

e_N for $\alpha\delta_i$, $i = 1, 2, 5$, and values of α in the range $-10 \le \alpha \le 10$. These re- sults were obtained after a slump time of $t = 0.1$ when there was full contact between the glass and former. Note that full contact is important; linearity is considerably worse where this is not achieved. The largest error at the centre ($|e_N| \sim 0.1$) corresponds to the case $i = 2$, $\alpha = 10$, and the sudden increase in error in the central region signals that we are entering a highly nonlinear zone. For other perturbations the error is very small at the centre and grows towards the edge. The increased error around $r \sim 0.8$ and beyond is an effect of the physical former edge.

Outside of the 'linear' response range, e_N depends in a complex manner on both the wavelength and amplitude of the perturbation, due to the differing ways in which the glass contacts the former. Excluding the error curve for $i = 2$, $\alpha = 10$, the results shown in Figures 4 and 5 are for a glass component that first contacts the former at the centre and then progressively from the centre up and the edge down. However, depending on the location and size of humps and holes in the former, initial contact may occur at some other position, significantly slowing the sag rate and resulting in different sequences of contact events, often with the result that full contact between glass and former is not achieved in the slump time. This, in turn, results in significantly different curvature profiles on the glass and much nonlinearity. The case $i = 2$, $\alpha = 10$, shown in Figure 5, is an example of such a change in the sequence of contact events, leading to a change in the nature of the error curve. To keep close to linear, the perturbation functions should be such that initial contact is at the centre of the former and the glass fully contacts the former in the slump time.

Next we consider perturbations $\alpha\delta_i + \beta\delta_j$, $i \ne j$ for which linearity is measured by $e_N = \mu_{i,\alpha;j,\beta} - \alpha\mu_i - \beta\mu_j$. Curvature perturbations for $i = 1$, $j = 2$ and $\alpha = \pm 1$, $\beta = \pm 1$ are given in Figure 6 and show a fair degree of symmetry, which is interesting. Plots for $i, j = 1, 5$ and $i, j = 2, 5$ show similar symmetry and curvature perturbations of a similar order of magnitude, although the curves, of course, differ significantly from those shown for $i, j = 1, 2$. The corresponding curves of e_N versus r for each of these i, j combinations are given in Figure 7, and show the error due to nonlinearity to be very small for these former perturbations. In general, the error will be worse where the effect of $\alpha\delta_i$ and $\beta\delta_j$ on the former is additive, which is most likely where α and β have the same sign. Hence in Figure 8 we look at the degree of nonlinearity for various values of $\alpha = \beta$. We find nonlinearity to increase significantly for some combinations of i, j with $\alpha = \beta$ smaller than -8 and larger than 6.

We have found a set of functions δ_i and range of coefficients α_i such that we expect a reasonably linear response to mould perturbations $\delta = \sum_i \alpha_i \delta_i$ to the base spherical former F_0, and hence we have reason to believe that our solution method will work for suitable choices of target and initial geometry. Of course,
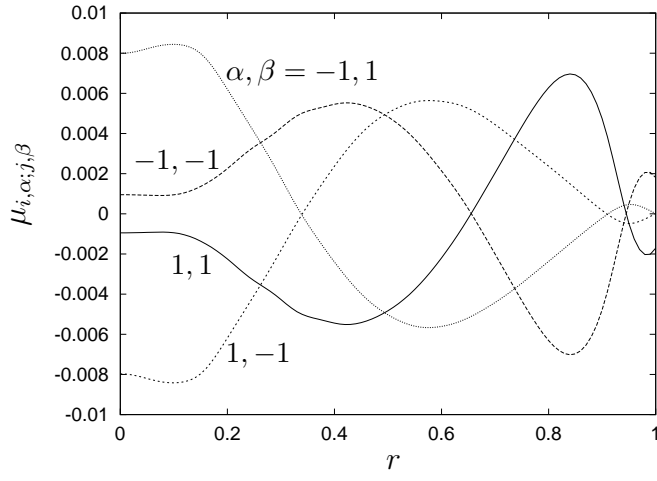
Fig. 6. Response $\mu_{i,\alpha;j,\beta}$ to former perturbations $\alpha\delta_i + \beta\delta_j$ for $i = 1$, $j = 2$ and $\alpha = \pm 1$, $\beta = \pm 1$.
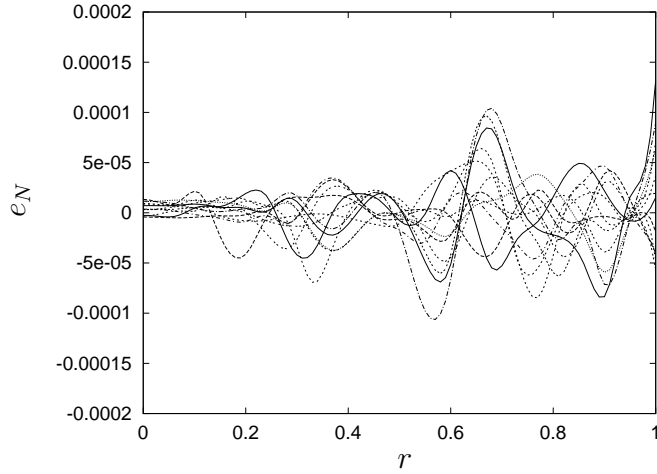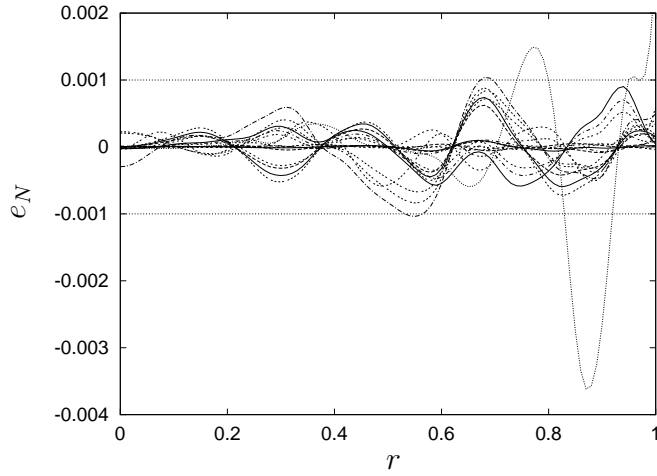

Fig. 7. Slumping of a pre-form of aspect ratio $h = 0.1333$ into a base spherical mould with $d = 0.05$. Error $e_N = \mu_{i,\alpha;j,\beta} - \alpha\mu_i - \beta\mu_j$ for $i, j = 1, 2; 1, 5; 2, 5$ and $\alpha = \pm 1$, $\beta = \pm 1$.

Fig. 8. Slumping of a pre-form of aspect ratio $h = 0.1333$ into a base spherical mould with $d = 0.05$. Error $e_N = \mu_{i,\alpha;j,\beta} - \alpha\mu_i - \beta\mu_j$ for $i, j = 1, 2; 1, 5; 2, 5$ and $\alpha = \beta = -8, -7, \pm 6, \pm 1$.

13

in practice, for given target, initial geometry and perturbation functions δ_i, we have no way to ensure that the coefficients α_i fall in the accepted linear range and, further, this range may change as the former shape is modified at each iteration. Hence, rather than be too concerned with the magnitude of the coefficients, we prefer to compute the error e_N due to nonlinearity at each iteration, which, at the mth iteration, is given exactly by

$$e_N = M_m - M_{m-1} - \sum_{i=1}^{m} \alpha_i \mu_i,$$

and is an easily computed measure of linearity; the closer to zero, the better is the linearity of the transfer function from former to glass.

Not all of the error in our method is due to nonlinearity. There is also a component e_L due to the least-squares fit to the target given, at the mth iteration, by

$$e_L = \sum_{i=1}^{m} \alpha_i \mu_i - \delta M_m = \sum_{i=1}^{m} \alpha_i \mu_i - (K - M_{m-1}).$$

The total error at iteration m is equal to the sum of these two components, i.e. $e_T = M_m - K = e_N + e_L = -\delta M_{m+1}$.

So far we have, somewhat arbitrarily, used the cosine functions (2) to define our former perturbation basis functions. This seems a natural choice, although there may be other suitable alternatives such as Bessel functions. Whatever we use, we must ensure enough degrees of freedom for our method to work while at the same time restricting the wavenumbers to the range that will be effectively transferable to the glass. This restriction on wavenumber is due to the fact that slumping smooths out small-scale perturbations on the former. Now, with the basis set (2) we must allow functions ranging up to large wavenumber so as to provide sufficient degrees of freedom for our method, which is clearly not satisfactory. Therefore, while continuing to use these functions to define the perturbations, we divide them into segments of one wavelength, each segment corresponding to a separate perturbation δ_i which adds a bump to the former surface for $\alpha_i > 0$ and a hole for $\alpha_i < 0$. This greatly increases the number of useful degrees of freedom available to us.

7   Example: Constant Curvature

We are now ready to use our method for an example problem. We continue to consider an initially flat glass disc with $h = 0.1333$ slumping into the initially spherical mould with $d = 0.05$, $R_f = 10.025$ which is the zeroth-order former solution for the desired constant curvature $K = 0.101095$ on the top surface

14

of the glass. The curvature profile M produced by this former is shown in Figure 2. We wish to modify the former shape to reduce the error in the curvature profile.

In our earlier linearity computations we saw the error increasing significantly around $r \sim 0.8$, an effect of the physical edge of the former. Hence, we choose to ignore the outer annular region and look to get closer to our target over the inner region $r \leq 0.8$. Thus, we choose our collocation points for determining the coefficients α_i in this range, taking 81 uniformly spaced points over $0 \leq r \leq 0.8$. We use as basis perturbation functions, segments of the cosine functions (2) with ϵ scaled as for the linearity calculations of the previous section. For the first six iterations, the orthogonalised curvature perturbations ν_i, $i = 1, \ldots, 6$ were obtained using the Gramm-Schmidt process just once. At this stage the relative magnitudes of the coefficients α_i, $i = 1, \ldots, 6$ indicated some loss of orthogonality between the ν_i and so the number of iterations of the Gramm-Schmidt process used to compute all of the ν_i was increased to two for iterations seven to twelve. For the same reason, the number of iterations of the Gramm-Schmidt process was increased to three at the thirteenth iteration which, however, failed to yield the desired dominant coefficient α_m with all other α_i, $i = 1, \ldots, (m-1)$, relatively small for $m \geq 13$. Computation was continued for twenty iterations, using twenty former-perturbation functions δ_i having wavelengths varying from the longest possible (i.e. the former diameter $= 2$) to one quarter of the former radius ($= 1/4$). These were ordered from longest to shortest wavelength and, within a set of perturbations of the same wavelength, the order was from the centre to the edge of the former.

Figure 9 shows the target for the next iteration δM_{m+1} at the end of iterations $m = 6$, 12 and 16. Also shown is the initial target ($m = 0$). The error components due to nonlinearity (e_N) and the least-squares fit (e_L) are given in Figures 10 and 11. Note that, at iteration m, $-\delta M_{m+1} = e_N + e_L$, the total error. We see a consistent decrease in the error due to the least-squares fit with increasing m (Figure 11) and this continues out to $m = 20$ where we ceased computation. By contrast, the error due to nonlinearity (Figure 10) remains quite small to $m = 12$ and then increases substantially; in fact this error component is larger at iterations $m = 13 - 15$ than that shown for $m = 16$. For further iterations ($m = 17 - 20$) this error component grows by several orders of magnitude. The effect of this, in combination with the decreasing least-squares error component, is that the total error (Figure 9) decreases to $m = 13$, increases for $m = 14$ and 15, decreases to the best overall result at $m = 16$ and then becomes very large at further iterations.

Nevertheless, while nonlinearity prevents further improvement on the results shown, at iterations $m = 12$ and 16 we have solutions that are a great improvement on the zeroth-order approximation.
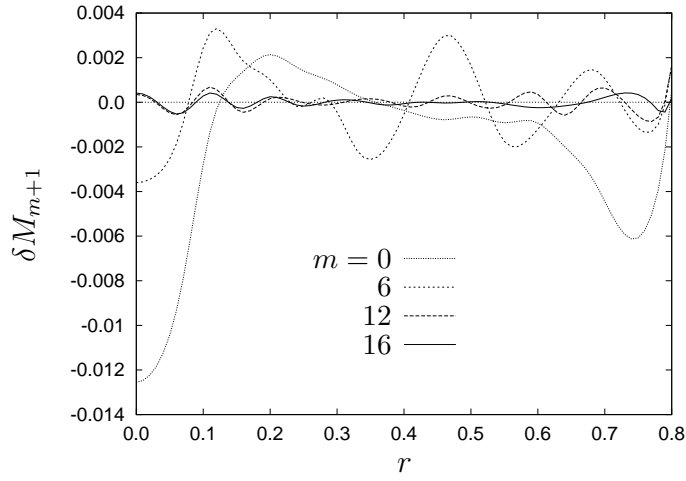
Fig. 9. Desired curvature $K = 0.101095$. New target $\delta M_{m+1} = K - M_m$, after iteration m; equivalently $-e_T$ where $e_T = e_N + e_L = M_m - K$ is the total error at iteration m.
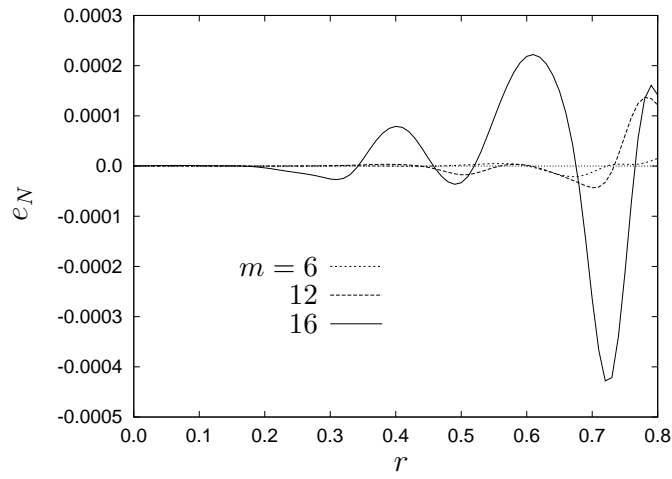

Fig. 10. Desired curvature $K = 0.101095$. Error due to nonlinearity $e_N = M_{m+1} - M_m - \sum_{i=1}^{m} \alpha_i \mu_i$, at iteration m.
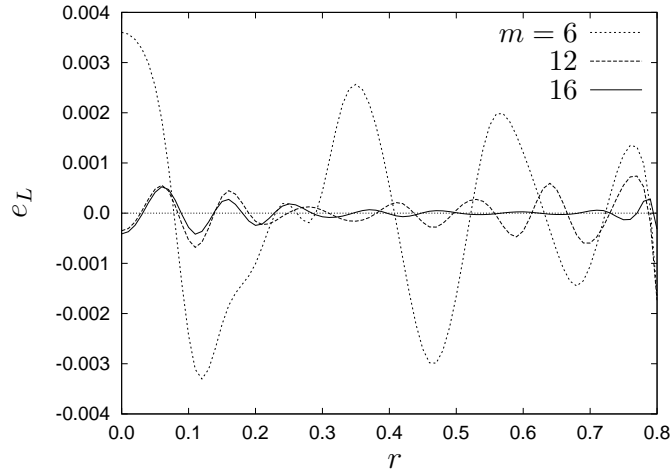

Fig. 11. Desired curvature $K = 0.101095$. Error due to least squares fit $e_L = \sum_{i=1}^{m} \alpha_i \mu_i - \delta M_m$, at iteration m.

16

8 Example: Quadratic Curvature

Obtaining a constant curvature on the glass by thermal replication is, practically speaking, unrealistic since there are better ways to obtain such a surface. Hence we consider the more realistic task of determining the former shape to give a quadratic curvature profile across the radius of the glass, with highest curvature in the centre, lowest curvature at the edge. Since we are taking curvature to be the second derivative, this means the former will be approximately described by a quartic polynomial. We consider the initial former elevation profile

$$F(r) = 0.05(r^2 - 1)(1 - 0.1r^2)$$

which gives a maximum cavity depth of $d = 0.05$ at the centre as for the spherical former already considered. We continue to use an initially flat glass disc with $h = 0.1333$ and we take $F(r)$ to be the zeroth-order former solution for the desired curvature profile on the glass $K = (F + h)''$, i.e. the quadratic curvature profile

$$K = 0.11 - 0.06r^2.$$

Note that this is a slightly different and less accurate definition of the zeroth-order solution than discussed earlier, obtained by simply translating the desired top surface of the glass vertically down by an amount equal to the glass thickness. Thus, we are starting with a less accurate estimate of the former geometry for our desired curvature profile compared to that used in the previous example.

Apart from the changed initial former geometry and desired curvature profile, we proceed exactly as for the previous example. Our results are shown in Figures 12–14. As for the constant curvature example considered first, an excellent solution is obtained after twelve iterations, after which error due to nonlinearity begins to grow and impact strongly on the results. As a result, the total error at $m = 13$ reduces a little compared to that at $m = 12$ but then increases substantially at $m = 14$. Depending on the importance of reducing error near $r = 0.8$, the solution at iteration $m = 15$ might be considered better than that at $m = 12$ or 13, but at subsequent iterations the error due to nonlinearity, and hence the total error, grows by several orders of magnitude.

The curves of new target δM_{m+1}, error due to nonlinearity e_N and error due to least-squares fitting e_L are quite similar in both appearance and magnitude for both examples, despite the fact that we started with a less accurate estimate of the solution for the quadratic-curvature case (compare the curves for $m = 0$, i.e. the initial error, in Figures 9 and 12). In both examples the growth in nonlinearity eventually prevents further improvment in the solution by including smaller wavelength perturbations in our basis set and continuing to iterate.
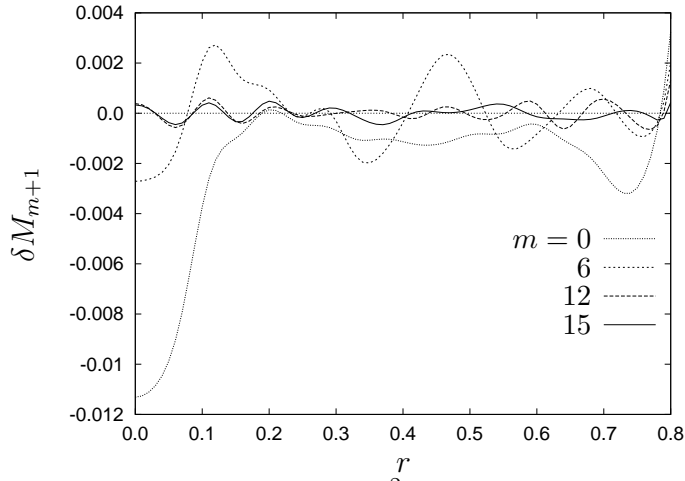
Fig. 12. Desired curvature $K = 0.11 - 0.06x^2$. New target $\delta M_{m+1} = K - M_m$, after iteration m; equivalently $-e_T$ where $e_T = e_N + e_L = M_m - K$ is the total error at iteration m.
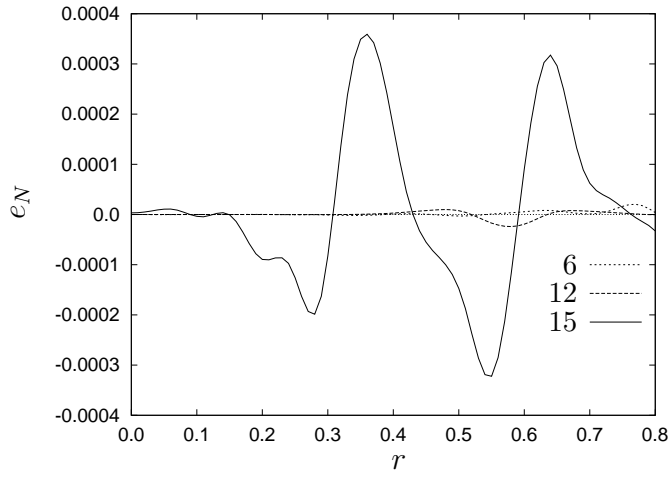

Fig. 13. Desired curvature $K = 0.11 - 0.06x^2$. Error due to nonlinearity $e_N = M_{m+1} - M_m - \sum_{i=1}^{m} \alpha_i \mu_i$, at iteration m.
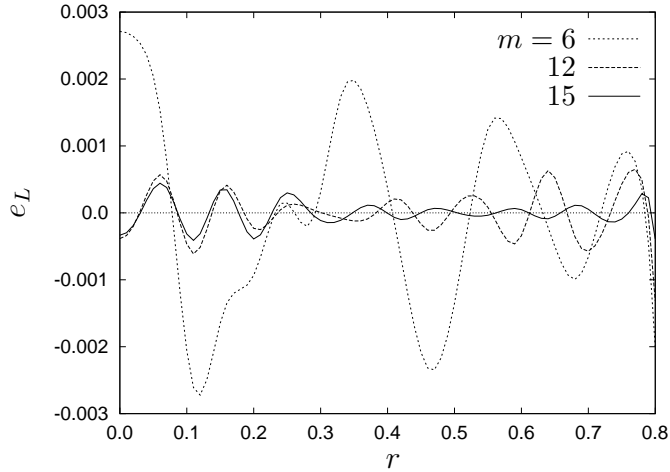

Fig. 14. Desired curvature $K = 0.11 - 0.06x^2$. Error due to least squares fit $e_L = \sum_{i=1}^{m} \alpha_i \mu_i - \delta M_m$, at iteration m.

18

9 Conclusions

We have applied the finite-element method to the Stokes Equation in order to solve the inverse problem of slumping of molten glass. This is a highly nonlinear problem. The slumping time required to achieve full contact, was determined first as achieving full contact between glass and former was found to be important to minimise nonlinearity. Then the shape of the ceramic former that produces a prescribed top surface curvature profile was sought, using a variant of the multivariable Newton-Raphson method. Choosing an appropriate set of basis perturbation functions for the former, a corresponding set of perturbation functions for the upper free surface of the glass is obtained by solving the forward slumping problem for each of the former perturbation functions. Then the lower former surface and desired upper free surface on the glass can be approximated by linear combinations of each of these sets of basis functions respectively. Thus the mapping is reduced to the finite-dimensional problem of solving for the set of coefficients in these linear combinations. Gramm-Schmidt orthogonalisation of the perturbation functions for the glass was carried out, to reduce the effect of nonlinear interaction.

We have studied the effect of the various parameters on the nonlinearity of this mapping. The nonlinearity was found to increase with the ratio of the glass thickness to the perturbation scale. Short-scale perturbations and thick glass, increase the nonlinearity. The steepness of the perturbation also increases nonlinearity. One of the challenges was to maintain a sufficient number of degrees of freedom to represent the required surfaces, while avoiding the strongly nonlinear short scales. This was achieved by introducing 'hump shaped' basis functions. These, being localized, also had (in general) less nonlinear interactions among them than, say, full cosine perturbations.

It is preferable to remove first the long-scale perturbations. These have larger amplitudes, for a given steepness, and behave more linearly. However, they interact in a strongly nonlinear way with shorter perturbations. Once the long-scale errors are reduced, the short-scale errors are easier to eliminate. Increasingly shorter-scale perturbations were gradually added.

The residual errors are largest near the outer edge of the former, which is usually trimmed in the industrial process. In fact, in addition to determining the former geometry to achieve the desired glass product, we can also determine the extent of edge trimming required for a given tolerance profile on the final product. Our results indicate that a trimming value of $r = 0.8$ is a reasonable choice.

This process reduced the error in curvature, within 12 iterations, from a magnitude of $1.3 \times 10^{-2} \, (1.1 \times 10^{-2})$ to $3.5 \times 10^{-4} \, (3.8 \times 10^{-4})$ at the centre and

$6.1 \times 10^{-3} \, (3.0 \times 10^{-3})$ to $6.2 \times 10^{-4} \, (4.3 \times 10^{-4})$ at $r = 0.75$ for the constant (quadratic) curvature case. After 12 iterations, the maximum error over $0 \leq r \leq 0.75$ was $6.2 \times 10^{-4} \, (6.3 \times 10^{-4})$ at $r = 0.75 \, (0.64)$ respectively; it increases to $1.6 \times 10^{-3} \, (1.3 \times 10^{-3})$ at $r = 0.8$ where trimming would almost certainly be appropriate. While these are excellent results, modifications may be required if there is need to further reduce the error, especially at shorter scales. Strategies for enhancing the method are currently being explored.

Acknowledgements

A   Computational algorithm

Final computational algorithm for determining the former $F(r, \theta)$ for the desired curvature profile $K(r, \theta)$:

1. Estimate/guess the former profile $F_0(r, \theta)$ that will yield K.
   $F_0(r, \theta) \Rightarrow M_0(r, \theta)$.
2. Do $m = 1, \, N$
2.1 Target $\delta M_m = K - M_{m-1}$.
2.2 If $|\delta M_m| <$ tolerance, $0 \leq r \leq b$ then stop.
2.3 Do $i = 1, \, m$
   (a) $F_{m-1} + \delta_i \Rightarrow M_{m-1} + \mu_i$.
   (b) Do j=1, $1(2, 3)$
       (i) $\nu_i \Leftarrow \mu_i, \, \gamma_i \Leftarrow \delta_i$
       (ii) Do $k = 1, \, (i - 1)$
       $$\nu_i \Leftarrow \nu_i - \frac{(\nu_i \cdot \nu_k)\nu_k}{\|\nu_k\|}, \qquad \gamma_i \Leftarrow \gamma_i - \frac{(\nu_i \cdot \nu_k)\gamma_k}{\|\nu_k\|}.$$
       (iii) $\delta_i \Leftarrow \gamma_i, \, F_{m-1} + \delta_i \Rightarrow M_{m-1} + \mu_i$
2.4 Solve $\delta M_m \approx \sum_{i=1}^{m} \alpha_i \mu_i$ for $\alpha_i, \, i = 1, \ldots, m$.
2.5 $F_m = F_{m-1} + \sum_{i=1}^{m} \alpha_i \delta_i$.
2.6 $F_m \Rightarrow M_m$

20

References

[1] F.M. Duarte and J.A. Covas, IR sheet heating in roll fed thermoforming Part 1 - Solving direct and inverse heating problems, Plast. Rubber Compos. 31 (2002) 307–317.

[2] F.M. Duarte and J.A. Covas, Infrared sheet heating in roll fed thermoforming Part 2 - Factors influencing inverse heating solution, Plast. Rubber Compos. 32 (2003) 32–39.

[3] H.W. Engl and P. Kugler, The influence of the equation type on iterative parameter identification problems which are elliptic or hyperbolic in the parameter, Eur. J. Appl. Math. 14 (2003) 129-163.

[4] P.D. Howell, Models for thin viscous sheets, Eur. J. Appl. Math. 9 (1998) 93–93.

[5] R. Hunt, Numerical solution of the flow of thin viscous sheets under gravity and the inverse windscreen sagging problem, Int. J. Numer. Meth. Fl. 38 (2002) 533-553.

[6] M. Hyre, Numerical simulation of glass forming and conditioning, J. Amer. Ceramic Soc. 85 (2002) 1047–1056.

[7] M.S. Joun and S.M. Hwang, Die shape optimal design in three-dimensional shape metal extrusion by the finite element method, Int. J. Numer. Meth. Eng. 42 (1998) 1343–1390.

[8] K. Laevsky and R.M.M. Mattheij, Determining the velocity as a kinematic boundary condition in a glass pressing problem, J. Comp. Meth. Sci. Eng. 2 (2003) 285–298.

[9] H.M. Pollicove, Survey of present lens molding techniques, In Riedl, M.J. (ed), Replication and Molding of Optical Components, Vol 896, Proceedings of The Society of Photo-Optical Instrumentation Engineers, Washington, 1988, pp. 158–159.

[10] H. Scholze and N.J. Kreidl, Technological aspects of viscosity, In Uhlmann, D.R. and Kreidl, N.J. (eds), Glass Science and Technology, Vol 3 Viscosity and Relaxation, Academic Press, Orlando, 1986, pp. 233–273.

[11] N. Siedow and M. Brinkmann, Direct and inverse temperature reconstruction of hot glass, in Proceedings of the 2nd International Colloquium "Modelling of Glass Forming and Tempering", Valenciennes 23 - 25 January 2002, pp. 173-177.

[12] L. Smith, R.J. Tillen and J. Winthrop, New directions in aspherics: glass and plastic, in Riedl, M.J. (ed), Replication and Molding of Optical Components, Vol 896, Proceedings of The Society of Photo-Optical Instrumentation Engineers, Washington, 1988, pp. 160–166.

[13] L.C. Sousa, C.F. Castro, C.A.C. Antonio and A.D. Santos, Inverse methods in design of industrial forging processes, J. Mater. Process. Tech. 128 (2002) 266–273.

[14] J. Sprekels, H. Goldberg and F. Tröltzsch, Numerical treatment of a shape optimization problem in thermoelasticity, DFG-Preprint series "Anwendungsbezogene Optimierung und Steuerung", Report No. 520.

[15] Y.M. Stokes, Thermal replication: a comparison of numerical and experimental results, in Tuck, E.O., Stott, J.A.K. (eds) Proceedings of the 3rd Biennial Engineering Mathematics and Applications Conference: EMAC98, Institution of Engineers, Australia, 1998, pp. 471–474.

[16] Y.M. Stokes, Very viscous flows driven by gravity with particular application to slumping of molten glass, PhD Thesis, Department of Applied Mathematics, University of Adelaide, July 1998.

[17] Y.M. Stokes, Numerical design tools for thermal replication of optical surfaces, Comput. Fluids 29 (2000) 401–414.

[18] E.O. Tuck, Y.M. Stokes and L.W. Schwartz, Slow slumping of a very viscous liquid bridge, J. Eng. Math. 32 (1997) 27–40.

[19] B.W. van de Fliert, P.D. Howell and J.R. Ockendon, Pressure-driven flow of a thin viscous sheet, J. Fluid Mech. 292 (1995) 359–376.

[20] C.H. Wang and H.F. Nied, Temperature optimization for improved thickness control in thermoforming, J. Mater. Process. Manu. 8 (1999) 113–126.

[21] X. Zhao, G. Zhao, G. Wang and T. Wang, Preform die shape design for uniformity of deformation in forging based on preform sensitivity analysis, J. Mater. Process. Tech. 128 (2002) 25–32.